Mild Acidosis Enhances AMPA Receptor-Mediated Intracellular Zinc Mobilization in Cortical Neurons

Valerio Frazzini,[1] Ilario G Rapposelli,[1] Carlo Corona,[1] Erica Rockabrand,[1] Lorella MT Canzoniero,[4] and Stefano L Sensi[1,2,3]

[1]Department of Basic and Applied Medical Science, Molecular Neurology Unit, CeSI-Center for Excellence on Aging, University 'G. d'Annunzio', Chieti, Italy; [2]Department of Neurology, University of California, Irvine, Irvine, CA, USA; [3]Department of Neurology, University of Texas Medical Branch, Galveston, Galveston, TX, USA; [4]Department of Biology and Environmental Sciences, University of Sannio, Benevento, Italy

Overactivation of glutamate receptors and subsequent deregulation of the intraneuronal calcium ((Ca^{2+})$_i$) levels are critical components of the injurious pathways initiated by cerebral ischemia. Another hallmark of stroke is parenchymal acidosis, and we have previously shown that mild acidosis can act as a switch to decrease NMDAR-dependent neuronal loss while potentiating the neuronal loss mediated by AMPARs. Potentiation of AMPAR-mediated neuronal death in an acidotic environment was originally associated only with (Ca^{2+})$_i$ dyshomeostasis, as assessed by Ca^{2+} imaging; however, intracellular dyshomeostasis of another divalent cation, Zn^{2+}, has recently emerged as another important co-factor in ischemic neuronal injury. Rises in (Zn^{2+})$_i$ greatly contribute to the fluorescent changes of Ca^{2+}-sensitive fluorescent probes, which also have great affinity for Zn^{2+}. We therefore revisited our original findings (Mcdonald et al., 1998) and investigated if AMPAR-mediated fura-2 signals we observed could also be partially due to (Zn^{2+})$_i$ increases. Fura-2 loaded neuronal cultures were exposed to the AMPAR agonist, kainate, in a physiological buffer at pH 7.4 and then washed either at pH 7.4 or pH 6.2. A delayed recovery of fura-2 signals was observed at both pHs. Interestingly this impaired recovery phase was found to be sensitive to chelation of intracellular Zn^{2+}. Experiments with the Zn^{2+} sensitive (and Ca^{2+}-insensitive) fluorescent probe FluoZin-3 confirmed the idea that AMPAR activation increases (Zn^{2+})$_i$, a phenomenon that is potentiated by mild acidosis. Additionally, our results show that selective Ca^{2+} imaging mandates the use of intracellular heavy metal chelators to avoid confounding effects of endogenous metals such as Zn^{2+}.

INTRODUCTION

Excitotoxicity is a key phenomenon that promotes neuronal demise in cerebral ischemia (1). Evidence cumulated in the past 30 years has linked ischemic neuronal death to the overactivation of glutamatergic ionotropic receptors (NMDA, N-Methyl-D-aspartate and AMPA, α-amino3-hydroxy-5-methyl-4-isoxazolepropionic-acid), a process that leads to massive Ca^{2+} entry into neurons and activation of a plethora of Ca^{2+}-dependent injurious pathways. NMDAR associated channels are highly Ca^{2+} permeable and seem to play a prominent role in ischemic neuronal death. Most of the AMPAR associated channels are Ca^{2+} impermeable; nevertheless, AMPAR activation is also able to mediate neurotoxic rises of intracellular Ca^{2+} ($[Ca^{2+}]_i$) via indirect opening of the voltage sensitive Ca^{2+} channels (VSCC). Parenchymal acidosis is another key component of the injurious pathways set in motion by cerebral ischemia (2), as well as an important modulator of excitotoxicity. NMDAR-mediated currents are attenuated by moderate extracellular acidity in the range of pH 6.2-7.2 (3–4), and in vitro, reduction of extracellular pH below 6.5 reduces both glutamate and oxygen-glucose deprivation induced neurotoxicity (5–7). While acidosis can reduce NMDAR-dependent neuronal loss, we previously have shown that lowering the extracellular pH can enhance AMPAR-mediated neuronal injury (8). Such enhanced toxicity originally was explained partially by increased $[Ca^{2+}]_i$ deregulation. In the Mcdonald study, we also found that neurons challenged with AMPA (under non-desensitizing conditions) undergo a phase of delayed recovery of $[Ca^{2+}]_i$ levels when washed in an acidic (pH 6.6) buffer. Using Ca^{2+} imaging experiments, this delayed recovery was attributed to deregulation of $[Ca^{2+}]_i$ homeostatic mechanisms, as evaluation of Ca^{2+} influx by $^{45}Ca^{2+}$ uptake showed that influx of the cation via VSCC was decreased by extracellular acidity.

Excitotoxic neuronal loss also has been linked to the dyshomeostasis of another divalent cation, Zn^{2+}. A large amount of data supports the idea that Zn^{2+} can in

fact act not only as a cellular messenger, but also as a potent trigger of neuronal death through several mechanisms – including energy depletion, reactive oxygen species (ROS) generation, and mitochondrial dysfunction, reviewed in (9). Injurious $[Zn^{2+}]_i$ rises have been linked to excitotoxic conditions such as transient global ischemia, head trauma, and epilepsy (10). Elevations of $[Zn^{2+}]_i$ are due to a combination of influx of the cation via glutamate receptors and VSCC activation, as well as its release from intracellular sites. Intracellularly Zn^{2+} is loosely bound to proteins such as metallothioneins (MTs) and several studies have indicated that the cation can be mobilized from MTs under conditions of oxidative stress. Further studies have shown that Zn^{2+} also can be mobilized in a Ca^{2+}-dependent fashion from mitochondria (11–12). Interestingly, changes in the intracellular proton concentration appear to act as a co-factor in ROS-mediated $[Zn^{2+}]_i$ rises as a decrease in pH rapidly destabilizes Zn^{2+} binding to MTs (13) and promotes an overall release of the cation. This phenomenon has now been confirmed in neurons, where mild acidosis has been found to dramatically increase $[Zn^{2+}]_i$ rises induced by MT oxidation (12).

A very intriguing debate has recently emerged in the excitotoxic field: the "Calcium- Zinc dilemma" (9,12,14–16). While for many years excitotoxicity has been interpreted as a purely Ca^{2+}-dependent process, most of the evidence for the Ca^{2+}-dependency derives from experimental paradigms that made use of either Ca^{2+} chelators or intracellular Ca^{2+} imaging with Ca^{2+} sensitive fluorescent indicators. One problem with this "Ca^{2+}-centered" view comes from the fact that both Ca^{2+} fluorescent probes and chelators also bind Zn^{2+}, and in fact do so with higher affinity. The potential confounding effect of Zn^{2+} on Ca^{2+} imaging has been neglected, moving from the assumption that $[Zn^{2+}]_i$ levels are very low. However, as mentioned above, a wealth of evidence has been gathered in recent years demonstrating that upon patho-

physiological conditions (i.e. oxidative and nitrosative stress; NMDAR activation and oxygen-glucose deprivation) $[Zn^{2+}]_i$ rises can reach levels high enough to greatly interfere with fluorescent measurements of $[Ca^{2+}]_i$ and/or chelation by divalent chelators (12,14,16–17). Thus, in this study, we critically re-examined our previous results (8) and investigated whether the AMPAR-mediated changes in fura-2 fluorescence signals that we originally interpreted as purely Ca^{2+}-dependent could be also linked to $[Zn^{2+}]_i$ rises.

MATERIALS AND METHODS

Materials

FluoZin-3 AM, fura-2 AM, and hydroethidine (Het) were purchased from Molecular Probes (Invitrogen, Milan, Italy). Carbonyl cyanide 3-chlorophenyl-hydrazone (CCCP), and *N,N,N′,N′*-Tetrakis-(2-pyridylmethyl)ethylene-diamine (TPEN) were obtained from Sigma-Aldrich (Milan, Italy). Tissue culture media and serum were from Gibco (Invitrogen, Milan, Italy). All other chemicals and reagents were obtained from common commercial sources.

Animal Cell Cultures

All animal procedures were approved by the institutional animal care and use committee. Murine cortical cultures were prepared from embryonic CD1 mice and neurons plated upon astrocytic monolayers on poly-lysine + laminin coated cover slips as previously described (18).

Fura-2, FluoZin-3, and HEt Microfluorimetric Studies

Fluorescence imaging was carried out using an inverted microscope with a xenon lamp, filter wheel, at 40X, epifluorescence oil immersion objective and fluorescent cubes. For ratiometric fura-2 imaging, cultures were loaded in the dark, with 3 μM of the acetoxymethyl ester form of the probe in a HEPES-buffered medium (HCSS) whose composition was (in mM): 120 NaCl, 5.4 KCl, 0.8 MgCl$_2$, 20 HEPES, 15 glucose, 1.8 CaCl$_2$, 10

NaOH, pH 7.4 for 30 min at 25°C, then washed in HCSS and kept in the dark for an additional 30 min, excitation was at 340 and 380 nm, with emission at 510 nm. For Zn^{2+} imaging, cells were loaded with the same protocol using 5 μM of FluoZin-3 AM, excitation was at 490 nm and emission at 530 nm. Experiments were carried out at room temperature (25°C). Drugs were applied by bath application and removed through a rapid flow exchange system. Images were acquired with a 12-bit digital CCD camera and analyzed (after background subtraction from a cell-free region of the dish) with Metafluor 6.0 software (Universal Imaging, West Chester, PA, USA).

Oxygen radical production was monitored using the oxidation sensitive dye, HEt. Stock HEt (1 mg/mL) was prepared as previously described (11) in dry DMSO and stored in frozen aliquots for use within eight weeks. Cultures were loaded in the dark with 5 μM HEt in HCSS (45 min, 25°C). After loading, cultures were washed (4×) in a static bath of HCSS containing 5 μM HEt. Cells were excited at 510–560 nm and emission monitored at > 590 nm.

Fura-2, FluoZin-3, and HEt fluorescence measurements for each cell (Fx) were normalized to either the fluorescence intensity (Fluozin-3 and HEt) or 340/380 ratio (fura-2) for that cell at the beginning of the experiment (F0) and changes over time expressed as percentage increase over baseline.

Experiment Replication and Statistics

All experiments reported represent at least three independent replications. Comparisons were obtained by Student-Newman-Keuls' test ($P < 0.01$).

RESULTS

We employed an experimental paradigm similar to the one used in our original study (8). Cortical neurons were loaded with the Ca^{2+}- (and Zn^{2+}-) sensitive ratiometric fluorescent probe fura-2 and fluorescence changes evaluated both during a 1 min exposure to 300 μM kainate and in the washout phase

(30 min at pH 7.4). At the end of the 30 min washout phase, neurons were exposed for 5 min to the cell-permeant heavy metal (and high affinity Zn^{2+}) chelator TPEN [20 μM; K_d 10^{-26} (19)]. In a second set of experiments, fura-2 fluorescence changes were investigated in neurons that, after the kainate challenge at pH 7.4, were washed in an acidic buffer (pH 6.2) for 30 min and then exposed to TPEN. Surprisingly, both in the case of post-kainate washout at pH 7.4 and pH 6.2, we observed a delayed recovery in the fura-2 signal. This delayed recovery in fura-2 fluorescence was found to be largely reduced upon TPEN exposure (Figure 1A and B). When we evaluated the extent of the decrease in the fura-2 signal produced by the TPEN exposure, we found no statistical difference between the two conditions. TPEN can decrease fura-2 fluorescence by 58% (SEM ± 4.33) in neurons washed at pH 7.4, while the same maneuver at pH 6.2 produced a 53% (SEM ± 2.68) fluorescence drop. When analyzing these $[Zn^{2+}]_i$ rises, one has to consider that potential differences could be difficult to be evaluated considering the high affinity for Zn^{2+} of fura-2 (K_d 0.5-3 nM).

To better analyze AMPAR-mediated $[Zn^{2+}]_i$ dyshomeostasis, we therefore loaded our cortical neurons with the Zn^{2+}-sensitive (and Ca^{2+}-insensitive) fluorescent probe FluoZin-3 (20). As with the fura-2 experiments, FluoZin-3 loaded neurons were imaged upon a brief excitotoxic pulse (300 μM kainate for 1 min at pH 7.4) and during a 20 min washout period either at pH 7.4 or pH 6.2 (Figure 2A and B). Integral analysis of $[Zn^{2+}]_i$ overload occurring in the washout period revealed that post-kainate Zn^{2+} dyshomeostasis is enhanced by extracellular acidosis (Figure 2C).

To elucidate the source of the $[Zn^{2+}]_i$ rises triggered by kainate exposure, we performed a control experiment in which FluoZin-3 loaded neurons were challenged with kainate and washed in an acidotic buffer in the presence of the extracellular Zn^{2+} chelator Ca^{2+}-EDTA (20 μM). Indicating that AMPAR activa-
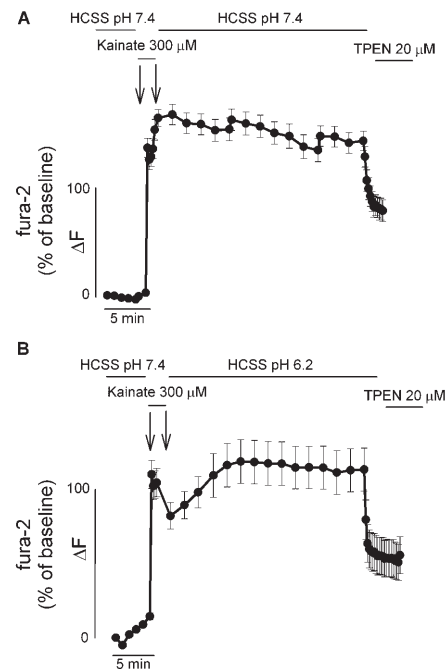
Figure 1. AMPAR activation increases both $(Ca^{2+})_i$ and $(Zn^{2+})_i$ levels. A, B. Time course of Ca^{2+} and Zn^{2+}-dependent changes in fura-2 fluorescence upon activation of AMPARs: Neuronal cultures loaded with fura-2 were imaged before, during, and after a 1 min exposure to 300 μM kainate. After the kainate challenge, neurons were washed for 30 min in a physiological buffer either at pH 7.4 (A) or pH 6.2 (B). At the end of the washout period, neurons were exposed for 5 min to the cell permeant Zn^{2+} chelator TPEN (20 μM). Traces show mean fura-2 ΔF (expressed as % over baseline of 340/380 nm ratios) (±SEM) of 13–24 neurons from one experiment representative of 5–6, respectively.

tion promotes a process of intracellular mobilization of Zn^{2+}, which is enhanced by low extracellular pH, chelation by Ca^{2+}-EDTA of any possible contaminant Zn^{2+} in the extracellular medium did not attenuate the FluoZin-3 fluorescent rises observed in the washout period (Figure 3A).

Mobilization of $[Zn^{2+}]_i$ can occur from MT oxidation as well as from Zn^{2+} release from mitochondria (12,14,17). We first explored the possibility that AMPAR
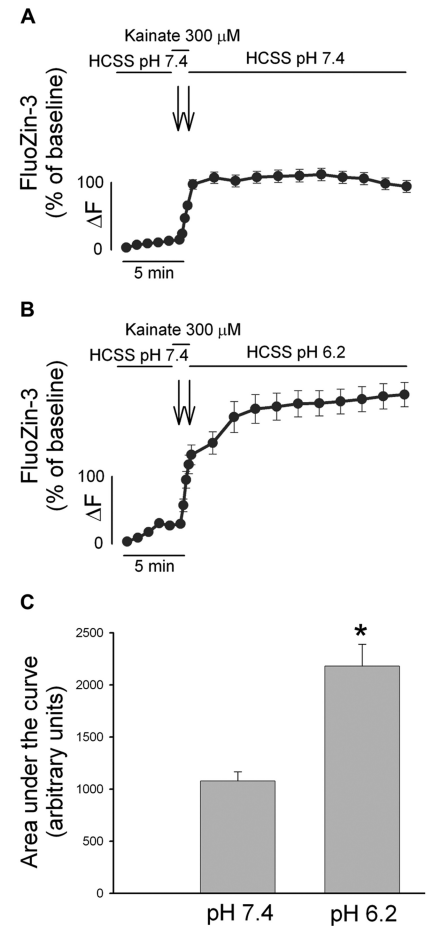
Figure 2. Mild acidosis enhances AMPAR-mediated $(Zn^{2+})_i$ rises. A, B. FluoZin-3 loaded cultures were exposed to kainate (300 μM) for 1 min and washed out in a physiological buffer either at pH 7.4 (A) or pH 6.2 (B) for 20 min. Traces show mean FluoZin-3 ΔF (±SEM) of > 50 neurons from 4–7 experiments. C. Bar graph depicts the area under the curve during the recovery phase in the two conditions, * indicates differences between washout at pH 7.4 versus washout at pH 6.2 ($P < 0.01$). Note that AMPAR-mediated $(Zn^{2+})_i$ rises are greatly enhanced upon exposure to an acidotic environment.

activation can induce release of Zn^{2+} present in mitochondria. In FluoZin-3 loaded cultures, exposure to a protonophore (CCCP; 1 μM) that collapses the mitochondrial membrane potential and, as shown before (11–12) promotes Zn^{2+}
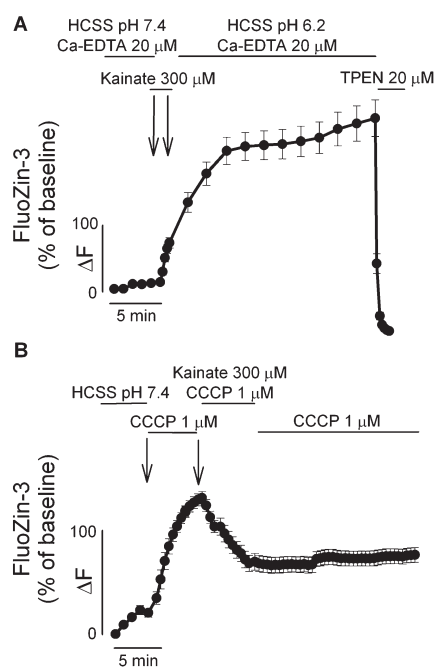
Figure 3. AMPAR-mediated $(Zn^{2+})_i$ rises are mainly dependent on intracellular Zn^{2+} mobilization. A. AMPAR-mediated $(Zn^{2+})_i$ rises are not modulated by extracellular Zn^{2+} chelation. FluoZin-3 loaded neurons were exposed, as in Figure 1, to kainate in the presence of the extracellular Zn^{2+} chelator Ca^{2+} EDTA (20 µM). Note that the $(Zn^{2+})_i$ rises occurring both during and after kainate exposure are not affected by extracellular chelation of contaminant Zn^{2+}, indicating that the source of these rises is intracellular. B. AMPAR-mediated release of intra-mitochondrial Zn^{2+}. FluoZin-3 loaded cultures were exposed for 5 min to the mitochondrial protonophore, CCCP (1 µM), challenged with 300 µM kainate for 5 min and washed at pH 7.4, in the presence of CCCP. Note that prior exposure to CCCP greatly inhibits subsequent kainate-triggered $(Zn^{2+})_i$ rises, indicating that these two manipulations target a common intracellular Zn^{2+} pool. Traces show time course of FluoZin-3 ΔF (±SEM), and are derived from > 15 neurons from 3–5 experiments.

release from mitochondria, produced a large increase in cytosolic FluoZin-3 fluorescence. Suggesting that mitochondria are a likely source for AMPAR-mediated $[Zn^{2+}]_i$ rises, CCCP exposure also oc-

cluded subsequent responses to kainate (Figure 3B).

On the contrary of NMDAR, AMPAR activation has been shown previously to generate very moderate oxidative stress of mitochondrial origin (21); therefore, a ROS-dependent Zn^{2+} mobilization seems less likely. We examined the possibility that AMPAR stimulation (at physiological and acidotic pH) can produce different levels of cytosolic ROS in neurons loaded with the superoxide sensitive fluorescent probe hydroethidine (HEt). Confirming the expected low oxidative stress produced by AMPAR activation under physiological conditions, Het-loaded neurons undergoing a 5 min kainate exposure showed very little increase in ROS production in the following 50 min when washed out in a buffer at pH 7.4 (Figure 4A). Interestingly, when the same excitotoxic challenge was followed by a 50 min wash at pH 6.2, ROS generation was found to be significantly higher (Figure 4B and C).

DISCUSSION

Our present study complements previous Ca^{2+} imaging studies in both neuronal cultures and hippocampal slices and clearly indicates that excitotoxic activation of glutamate receptors leads not only to $[Ca^{2+}]_i$ dyshomeostasis but also to a significant $[Zn^{2+}]_i$ mobilization. This idea is substantiated by the interpretation of the increases in both fura-2 ratios and FluoZin-3 fluorescence (quenched by TPEN) that we observed. Fura-2 has a low affinity for Mg^{2+} (K_d 6–10 mM) and exhibits an affinity for Zn^{2+} that is nearly 100-fold higher than its affinity for Ca^{2+} (K_d 0.5–3 nM). Upon Zn^{2+} binding, fura-2 fluorescence undergoes changes similar to what is observed with Ca^{2+} (i.e. increases of the 340/380 nm excitation ratio). On the other hand, fura-2 binding to transition metals likely to be intracellularly released in significant amounts, such as manganese, ferrous and ferric iron, and copper results in different levels of quenching of the probe fluorescence.
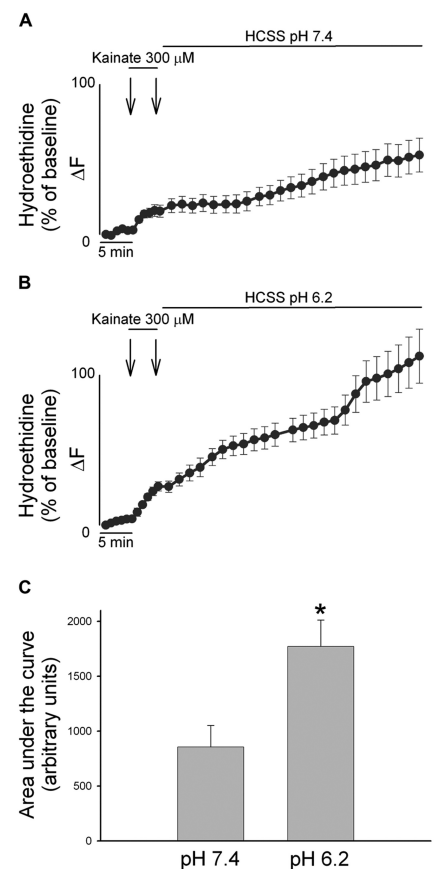
Figure 4. AMPAR-mediated ROS generation is enhanced by low extracellular pH. A, B. Cortical cultures were loaded with HEt, and exposed for 5 min to 300 µM kainate and washed for 50 min with a buffer at pH 7.4 (A) or pH 6.2 (B). HEt fluorescence changes for each neuron are expressed as the ratio of fluorescence at each time point (F_x) to its own baseline fluorescence (F_0). Traces show mean (± SEM) of 29 (A) or 40 (B) neurons from 3 experiments. C. Bar graph depicts the cumulative ROS production as area under the curve during the recovery phase in the two conditions, * indicates differences between washout at pH 7.4 versus washout at pH 6.2 ($P < 0.01$) Note the marked increase in HEt fluorescence only in the case of kainate exposures followed by an acidotic wash out.

FluoZin-3 is a Zn^{2+} selective indicator that exhibits high Zn^{2+} binding affinity (K_d for Zn^{2+} ~15 nM), that is unperturbed by Ca^{2+} and Mg^{2+} concentrations up to at

least 0.1 mM and 1 M respectively (20). As with fura-2, iron and copper binding to FluoZin-3 produce quenching of the probe fluorescence. Thus, the only metal that could promote TPEN-sensitive increases in both fura-2 ratios and FluoZin-3 fluorescence is Zn^{2+}.

Our findings reinforce the idea that glutamate receptor overactivation can trigger a synergistic injurious interplay between Ca^{2+} and Zn^{2+}. Considering the fact that Zn^{2+} is able to induce neuronal loss with greater potency compared with Ca^{2+}, the cation might soon emerge as the major ionic determinant of excitotoxicity. Indeed, given the fact that significant $[Zn^{2+}]_i$ release from mitochondria can result from large, NMDAR-triggered $[Ca^{2+}]_i$ rises, and the likely probability that Ca^{2+}-induced mitochondrial ROS generation could also trigger Zn^{2+} mobilization from MTs, we might envision a pathological setting in which glutamate receptor-driven $[Ca^{2+}]_i$ rises actually play a more modest injurious role than previously thought. Instead of being the executioner, $[Ca^{2+}]_i$ dyshomeostasis can actually serve as an "accomplice" to deregulate the intracellular concentrations of the primary ionic mediator of neuronal injury, Zn^{2+}.

This study also integrates the main results of our previous experiments with the novel finding that reduction of extracellular pH to levels of parenchymal acidosis associated with cerebral ischemia (2) enhances AMPAR-mediated Zn^{2+} dyshomeostasis.

The connection between Zn^{2+} and acidosis is intriguing as pH reduction can affect many Zn^{2+} homeostatic systems. The permeability of major routes of Zn^{2+} entry, such as the VSCC and Ca^{2+}-permeable AMPAR, is enhanced at acidic pH, while the Ca^{2+} permeability of these channels (as well as NMDAR permeability) has been shown to be decreased under the same conditions (22–23). Zn^{2+} uptake and compartmentalization by Zinquin-positive cytosolic organelles is blocked by intracellular acidification, indicating the presence of a putative intracellular Zn^{2+}/proton

antiporter (24), and previous studies have also indicated that an acidotic environment can greatly destabilize Zn^{2+} binding to MTs and therefore promote $[Zn^{2+}]_i$ accumulation (13). Interestingly, Zn^{2+} dyshomeostasis itself can alter the intracellular acid-base equilibrium and promote a feed-forward dyshomeostatic loop. Findings in cultured neurons suggest that Zn^{2+} can in fact favor intracellular acidification in a Ca^{2+}-dependent fashion through an increased activity of the Na^+/Ca^{2+} exchanger, and also maintain such acidification by Zn^{2+}-dependent inhibition of proton efflux via the Cl^-/HCO_3^- exchanger (25). Finally, as observed in our study, prolonged intracellular acidosis could further evoke $[Zn^{2+}]_i$ dyshomeostasis by interfering with the overall neuronal redox state, either by reducing the activity of cellular antioxidant enzymes or increasing hydroxyl radical formation (26).

In our study, it appears that the acidotic/AMPAR-mediated $[Zn^{2+}]_i$ rises observed in neuronal cultures can be attributed to combined mechanisms of mitochondrial release of the cation together with impaired buffering by MTs. The fact that mitochondrial depolarization prior to the kainate exposure completely occludes AMPAR-mediated $[Zn^{2+}]_i$ increases seems to indicate that most of the Zn^{2+} is released from that subcellular compartment (Figure 3B). On the other hand, the impaired Zn^{2+} buffering under acidotic conditions that follows AMPAR activation appears to be related to a synergistic inhibition on Zn^{2+} binding to MTs that is promoted by protons either directly (13), or indirectly, by enhancing AMPAR-mediated ROS production. This process eventually leads to MT oxidation and further decreased Zn^{2+} buffering.

On a speculative note, our model, which emphasizes the role played by acidosis and AMPAR-mediated Zn^{2+} dyshomeostasis in excitotoxicity, might be relevant for the timing and selection of pharmacological intervention in neurological conditions associated with both acidosis and alteration of $[Zn^{2+}]_i$ content

such as stroke, status epilepticus, and trauma. While hours away from the ischemic attack when the acid-base equilibrium is restored, NMDAR antagonists maintain a very important therapeutic value, AMPAR antagonists might result as a better option immediately after the insult given the fact that NMDARs are already blocked by post-ictal parenchymal acidosis (27). The importance of AMPAR antagonism has been demonstrated recently by an elegant series of studies in which blockade of the Ca^{2+}-permeable AMPARs has been found to be neuroprotective both in "in vitro" and "in vivo" models of cerebral ischemia (28–30). Work by our laboratory and the groups of Suzanne Zukin and Mike Bennett has convincingly demonstrated that, in the post-ischemic period, blockade of Ca-A/K channels by spermine derivatives can greatly inhibit neuronal death in the CA1 hippocampal region by counteracting both $[Zn^{2+}]_i$ accumulation and Zn^{2+}-dependent injurious processes.

Targeting Zn^{2+} dyshomeostasis might also require further exploration, as recent animal studies involving the use of pyruvate to restore Zn^{2+}-dependent injurious depletion of cytosolic NAD^+ levels showed a dramatic neuroprotective effect in the context of both global and focal cerebral ischemia (31–32).

A final technical issue raised by our findings concerns the need for highly selective Ca^{2+}-sensitive fluorescent probes. The warning contained in the paper by Grynkiewicz, Poenie and Tsien (33) indicating the high sensitivity of Ca^{2+}-sensitive fluorescent probes to heavy metals has been neglected. It is now clear that mobilization of intracellular Zn^{2+} can be a significant contributor to the fluorescence changes of Ca^{2+} fluorescent probes. This effect should no longer be ignored nor Ca^{2+} dependency claimed without a prior careful exclusion of Zn^{2+}-dependent phenomena.

REFERENCES

1. Lee JM, Zipfel GJ, Choi DW. (1999) The changing landscape of ischaemic brain injury mechanisms. *Nature*. 399:A7–14.

2. Chesler M. (2003) Regulation and modulation of pH in the brain. *Physiol. Rev.* 83:1183–221.

3. Tang CM, Dichter M, Morad M. (1990) Modulation of the N-methyl-D-aspartate channel by extracellular H+. *Proc. Natl. Acad. Sci. U. S. A.* 87:6445–9.

4. Traynelis S, Cull-Candy S. (1990) Proton inhibition of N-methyl-D-aspartate receptors in cerebellar neurons. *Nature*. 345:347–50.

5. Giffard RG, Monyer H, Christine CW, Choi DW. (1990) Acidosis reduces NMDA receptor activation, glutamate neurotoxicity, and oxygenglucose deprivation neuronal injury in cortical cultures. *Brain Res*. 506:339–42.

6. Tombaugh GC, Sapolsky RM. (1990) Mild acidosis protects hippocampal neurons from injury induced by oxygen and glucose deprivation. *Brain Res*. 506:343–5.

7. Kaku DA, Giffard RG, Choi DW. (1993) Neuroprotective effects of glutamate antagonists and extracellular acidity. *Science*. 260:1516–8.

8. McDonald JW et al. (1998) Extracellular acidity potentiates AMPA receptor-mediated cortical neuronal death. *J. Neurosci*. 18:6290–9.

9. Sensi SL, Jeng JM. (2004) Rethinking the excitotoxic ionic milieu: the emerging role of $Zn^{(2+)}$ in ischemic neuronal injury. *Curr. Mol. Med*. 4:87–111.

10. Frederickson CJ, Koh JY, Bush AI. (2005) The neurobiology of zinc in health and disease. *Nat. Rev. Neurosci*. 6:449–62.

11. Sensi SL, Ton-That D, Weiss JH. (2002) Mitochondrial sequestration and $Ca^{(2+)}$-dependent release of cytosolic $Zn^{(2+)}$ loads in cortical neurons. *Neurobiol. Dis*. 10:100–8.

12. Sensi SL et al. (2003) Modulation of mitochondrial function by endogenous Zn^{2+} pools. *PNAS*. 100:6157–62.

13. Jiang LJ, Vasak M, Vallee BL, Maret W. (2000) Zinc transfer potentials of the alpha- and beta-clusters of metallothionein are affected by domain interactions in the whole molecule. *Proc. Natl. Acad. Sci. U. S. A.* 97:2503–8.

14. Bossy-Wetzel E et al. (2004) Crosstalk between nitric oxide and zinc pathways to neuronal cell death involving mitochondrial dysfunction and p38-activated K+ channels. *Neuron*. 41:351–65.

15. Devinney MJ, 2nd, Reynolds IJ, Dineley KE. (2005) Simultaneous detection of intracellular free calcium and zinc using fura-2FF and FluoZin-3. *Cell Calcium*. 37:225–32.

16. Stork CJ, Li YV. (2006) Intracellular zinc elevation measured with a "calcium-specific" indicator during ischemia and reperfusion in rat hippocampus: a question on calcium overload. *J. Neurosci*. 26:10430–7.

17. Aizenman E et al. (2000) Induction of neuronal apoptosis by thiol oxidation: putative role of intracellular zinc release. *J. Neurochem*. 75:1878–88.

18. Yin HZ, Weiss JH. (1995) $Zn^{(2+)}$ permeates $Ca^{(2+)}$ permeable AMPA/kainate channels and triggers selective neural injury. *Neuroreport*. 6:2553–6.

19. Arslan P, Di Virgilio F, Beltrame M, Tsien RY, Pozzan T. (1985) Cytosolic Ca^{2+} homeostasis in Ehrlich and Yoshida carcinomas. A new, membrane-permeant chelator of heavy metals reveals that these ascites tumor cell lines have normal cytosolic free Ca^{2+}. *J. Biol. Chem*. 260:2719–27.

20. Gee KR, Zhou ZL, Ton-That D, Sensi SL, Weiss JH. (2002) Measuring zinc in living cells. A new generation of sensitive and selective fluorescent probes. *Cell Calcium*. 31:245–51.

21. Dugan LL et al. (1995) Mitochondrial production of reactive oxygen species in cortical neurons following exposure to N-methyl-D-aspartate. *J. Neurosci*. 15:6377–88.

22. Kerchner G, Canzoniero L, Yu S, Ling C, Choi DW. (2000) Zn^{2+} current is mediated by voltage-gated Ca^{2+} channels and enhanced by extracellular acidity in mouse cortical neurones. *J. Physio* . 528:39–52.

23. Jeng J-M, Jia, Y., Bonanni, L., Weiss, J.H. (2002) Divergent effects of pH on Zn^{2+} and Ca^{2+} flux through Ca^{2+}-permeable AMPA/kainate channels (CAKR) *SFN Annual Meeting*. Washington, DC: Society for Neuroscience, Orlando, FL, p.539.

24. Colvin RA. (2002) pH dependence and compartmentalization of zinc transported across plasma membrane of rat cortical neurons. *Am. J. Physiol. Cell Physiol*. 282:C317–29.

25. Dineley KE, Brocard JB, Reynolds IJ. (2002) Elevated intracellular zinc and altered proton homeostasis in forebrain neurons. *Neuroscience*. 114:439–49.

26. Ying W, Han SK, Miller JW, Swanson RA. (1999) Acidosis potentiates oxidative neuronal death by multiple mechanisms. *J. Neurochem*. 73:1549–56.

27. Gill R, Lodge D. (1997) Pharmacology of AMPA antagonists and their role in neuroprotection. *Int. Rev. Neurobiol*. 40:197–232.

28. Yin HZ, Sensi SL, Ogoshi F, Weiss JH. (2002) Blockade of Ca^{2+}-permeable AMPA/kainate channels decreases oxygen-glucose deprivation-induced Zn^{2+} accumulation and neuronal loss in hippocampal pyramidal neurons. *J. Neurosci*. 22:1273-1279.

29. Calderone A et al. (2004) Late calcium EDTA rescues hippocampal CA1 neurons from global ischemia-induced death. *J. Neurosci*. 24:9903–13.

30. Noh KM et al. (2005) Blockade of calcium-permeable AMPA receptors protects hippocampal neurons against global ischemia-induced death. *Proc. Natl. Acad. Sci. U. S. A.* 102:12230–5.

31. Lee JY, Kim YH, Koh JY. (2001) Protection by pyruvate against transient forebrain ischemia in rats. *J. Neurosci*. 21:RC171.

32. Yi JS, Kim TY, Kyu Kim D, Koh JY. (2007) Systemic pyruvate administration markedly reduces infarcts and motor deficits in rat models of transient and permanent focal cerebral ischemia. *Neurobiol. Dis*. 26:94–104.

33. Grynkiewicz G, Poenie M, Tsien RY. (1985) A new generation of Ca^{2+} indicators with greatly improved fluorescence properties. *J. Biol. Chem*. 260:3440–50.